ground water

Analysis of Karst Aquifer Spring Flows with a Gray System Decomposition Model

by Yonghong Hao[1,2], Tian-Chyi J. Yeh[3], Yanrong Wang[2], and Ying Zhao[4]

Abstract

There are ~470,000 km^2 of karst aquifers that feed many large springs in North China. Turbulent flow often exists in these karst aquifers, which means that the classical ground water model based on Darcy's law cannot be applied here. Ground water data are rare for these aquifers. As a consequence, it is difficult to quantitatively investigate ground water flow in these karst systems. The purpose of this study is to develop a parsimonious model that predicts karst spring discharge using gray system theory. In this theory, a white color denotes a system that is completely characterized and a black color represents a system that is totally unknown. A gray system thus describes a complex system whose characteristics are only partially known or known with uncertainty. Using this theory, we investigated the karst spring discharge time series over different time scales. First, we identified three specific components of spring discharge: the long-term trend, periodic variation, and random fluctuation. We then used the gray system model to simulate the long-term trend and obtain periodic variation and random fluctuation components. Subsequently, we developed a predictive model for karst spring discharge. Application of the model to Liulin Springs, a representative example of karst springs in northern China, shows that the model performs well. The predicted results suggest that the Liulin Springs discharge will likely decrease over time, with small fluctuations.

Introduction

Karst aquifers are highly heterogeneous in nature. They are dominated by secondary or tertiary porosity (i.e., fractures or conduits, respectively) and may exhibit hierarchical permeability structures or flowpaths (Labat et al. 1999). Furthermore, behavior of water flow in karst aquifers is likely to be turbulent, and problematic for models based on Darcy's law, which assumes laminar flow (White 1988, 2002; Zhang et al. 1996; Scanlon et al. 2003). Quinlan et al. (1996) stated that "numerical models applied to karstic terranes have frequently failed. The current approach used most commonly is the single continuum porous media flow characterization typified by MODFLOW. The reality is that karst systems are double or triple porosity systems where both laminar and turbulent flow occur, and flow may even change from one to the other with time."

Despite the aforementioned difficulties, two modeling approaches have commonly been used to investigate ground water resources in karst aquifers. One approach (a black box approach) relies on the input-output relation, treating the aquifer as a black box (Dreiss 1982). That is, it uses an empirical relation to investigate the properties of the karst aquifer, such as an exponential decay of a spring hydrograph following precipitation. This established empirical relation, however, may change with time or events, and its predictive ability is rather limited. The second approach uses a physically based model that relates physical karst features, such as constricted passages and high-flow springs, to fluid mechanics (Haliham et al. 1998; Barfield et al. 2004). This physically based model is quite difficult to use because it requires detailed information about the characteristics of the flow system

[1]Corresponding author: Department of Hydrology and Water Resources, The University of Arizona, Tucson, AZ 85721; (520) 621-2842; fax: (520) 621-1422; yhao@hwr.arizona.edu

[2]School of Environment and Resources, Shanxi University, Taiyuan, 030006 Shanxi Province, People's Republic of China.

[3]Department of Hydrology and Water Resources, The University of Arizona, Tucson, AZ 85721.

[4]Research Center of Environmental Science and Engineering, Shanxi University, Taiyuan, Shanxi Province, People's Republic of China.

Received March 2006, accepted June 2006.

doi: 10.1111/j.1745-6584.2006.00255.x

(boundary conditions, porosity, hydraulic conductivity, three-dimensional extent of the aquifer, etc.), and such data are generally unavailable, particularly for a large karst ground water basin (Labat et al. 1999, 2000; Long and Derickson 1999; Majone et al. 2004).

Almost 10% of the landmass of China is karst terrain, concentrated in two regions: an area of ~470,000 km^2, located in a semiarid climate zone in the northern part of China, and a humid climate zone in the southwest part of China, an area of ~500,000 km^2 (Yuan 1994). Differences in precipitation amount have created different karst hydrological properties in these two karst regions. In semiarid areas, caves and subsurface rivers are not typically present and the karst aquifer is dominated by fissures, fractures, and conduits. In contrast, the karst systems in humid regions are characterized by well-developed caves and highly connected underground flow channels (Yuan 1994). In the semiarid areas, the ratios of maximum to minimum spring flow generally range from 1.24 to 5.89, whereas the ratios are from 10 to 1000 in the humid regions (He et al. 1997). The contrast in the ratios of the two regions is indicative of karst aquifers' slow response to precipitation in the semiarid regions. Moreover, in semiarid regions the pores, fissures, and fractures provide extensive storage for precipitation, and ground water often discharges as karst springs within basins of thousands of square kilometers (Han et al. 1993; Ma et al. 2004). In contrast, karst aquifers in humid regions have caves connected by channels and subsurface rivers where ground water residence time is short and storage for precipitation is small. Thus, in the semiarid regions, karst ground water is the major source of the water supply.

Generally, management and conservation strategies do not exist for ground water resources in the semiarid region of northern China. Information about ground water availability is also scarce. Nevertheless, the discharge observed from most karst springs has been declining over the past few decades, and some have even become completely dry. Therefore, there is an urgent need for investigation of the karst ground water resources in this semiarid region. Because of limited data and the complicated nature of karst aquifers, the aim of this study is to develop a parsimonious model that predicts karst spring discharge using gray system theory. As a representative of karst springs in North China, the Liulin Springs were selected as our study area. Different from the work by Hao et al. (2006), which focused on the response of springs to climatic change, this paper investigates the variability of spring flow over time. The previous study indicated that the karst ground water residence time in Liulin Spring basin is ~4 years and the karst aquifers respond remarkably to climate changes, in particular to changes in precipitation input.

Simulation of Karst Spring Discharge Based on a Gray System Model

In gray system theory, a white color denotes a system that is completely characterized and a black color represents a system that is totally unknown. A gray system describes a complex system whose characteristics are only partially known or known with uncertainty (Deng 1982, 1985). In karst systems, precipitation and runoff become ground water by infiltration through the vadose zone, or through sinkholes, fractures, etc. In the subsurface, water flows through the porous matrix, fissures, fractures, or conduits and may emerge as springs. It is a complex process. Based on the ideas of gray system theory, the karst ground water system is more accurately viewed as a gray system where part of the information is clearly known (e.g., spring discharge) and part is obscure (e.g., variability of fissures and conduits) (Lee and Wang 1998; Xia 2000).

Examining the karst spring discharge data over different time scales, we found that it has different trends. The time series of spring flow $Q(t)$ generally includes three specific components at different time scales: (1) the long-term trend, $\hat{x}^{(0)}(t)$; (2) periodic variation, $S(t_i)$; and (3) random fluctuation, $R(t)$.

When the water table rises, spring discharge will increase, and if ground water levels fall, spring discharge decreases (White 1988). Over a long period of time, a water table may exhibit a general trend, either ascending or descending, and spring discharge responds accordingly.

Spring discharge also shows periodic changes over shorter intervals. The two primary factors that lead to short-term fluctuations are short-term climate variation in the karst ground water basin and human activities (e.g., ground water pumping).

In addition to the long-term and periodic behaviors in the spring discharge time series, the spatial distribution of meteorological and vegetation factors and, perhaps, spatial heterogeneity of the aquifer may cause the small-scale fluctuations in spring discharge. Fluctuations of spring discharge at this scale are described as random fluctuations.

Based on this conceptualization, spring discharge can thus be expressed as

$$Q(t) = \hat{x}^{(0)}(t) + S(t_i) + R(t) \qquad (1)$$

where $Q(t)$ is defined as the spring discharge, $\hat{x}^{(0)}(t)$ the long-term trend of the spring flow, $S(t_i)$ the periodic variation, and $R(t)$ the random fluctuation.

We use a gray system GM(1,1) model to simulate the long-term trend. By analyzing the residuals of the long-term trend, we obtain periodic variation and random fluctuation components.

Structure and Behavior of the GM(1,1) Model

GM(1,1) means a gray model with first order differential time series equations in one variable. The differences between the GM(1,1) model, autoregressive integrated moving average models, and other time series analysis methods are that the gray system theory does not rely on temporal correlation or cross-correlation (i.e., statistics) as in time series analysis of the Western-world statistical literature, and GM(1,1) is set up using data transformed from an accumulating generation. In such a transformation, assume that

$$X^{(0)} = (x^{(0)}(1), x^{(0)}(2), \ldots, x^{(0)}(n)) \quad (2)$$

is a time series of raw data.

$$x^{(1)}(t) = \sum_{i=1}^{t} x^{(0)}(i), t = 1, 2, \ldots, n \quad (3)$$

is regarded as the accumulating generation and

$$X^{(1)} = (x^{(1)}(1), x^{(1)}(2), \ldots, x^{(1)}(n)) \quad (4)$$

is the transformed data series of $X^{(0)}$.

Through accumulation, the development situation and tendency of $X^{(0)}$ can be seen so that any special characteristics or laws, hidden in the chaotic raw data, can be sufficiently revealed (Liu and Lin 1998).

In gray system theory, the $X^{(0)}$ and $X^{(1)}$ are defined as gray quantities. The gray derivative of $x^{(1)}$ is given by

$$\frac{\mathrm{d}x^{(1)}(t)}{\mathrm{d}t} = \frac{x^{(1)}(t) - x^{(1)}(t-1)}{t - (t-1)} = x^{(0)}(t) \quad (5)$$

and then the equation,

$$x^{(0)}(t) + ax^{(1)}(t) = b \quad (6)$$

gives us an equation of the gray differential type. If we replace $x^{(1)}(t)$ in Equation 6 by the new background value,

$$z^{(1)}(t) = 0.5x^{(1)}(t) + 0.5x^{(1)}(t-1),\ t = 1, 2, \ldots, n \quad (7)$$

then $z^{(1)}(t)$ and the components $x^{(1)}(t)$ and $x^{(1)}(t-1)$ of the gray derivative satisfy the crucial arithmetical horizontal mapping relation, and Equation 6 becomes the governing gray differential equation in our GM(1,1) model (Liu and Lin 1998; Liu et al. 2004):

$$x^{(0)}(t) + az^{(1)}(t) = b \quad (8)$$

If we let

$$Y = \begin{bmatrix} x^{(0)}(2) \\ x^{(0)}(3) \\ \ldots \\ x^{(0)}(n) \end{bmatrix} \quad (9)$$

and let

$$B = \begin{bmatrix} -z^{(1)}(2), 1 \\ -z^{(1)}(3), 1 \\ \ldots\ldots \\ -z^{(1)}(n), 1 \end{bmatrix} \quad (10)$$

then the least square estimates of a and b from Equation 8 are given by

$$(a, b)^T = (B^T B)^{-1} B^T Y \quad (11)$$

Using these estimates of a and b, our "whitenizing" equations of the gray system (Equation 8) are given by

$$\frac{\mathrm{d}x^{(1)}(t)}{\mathrm{d}t} + ax^{(1)}(t) = b \quad (12)$$

The solution of Equation 12 can be readily found as

$$x^{(1)}(t) = (x^{(1)}(0) - \frac{b}{a})\mathrm{e}^{-at} + \frac{b}{a} \quad (13)$$

Then the approximate time response sequences of the GM(1,1) gray differential system (Equation 8) are set up as

$$\hat{x}^{(1)}(t+1) = (x^{(1)}(0) - \frac{b}{a})\mathrm{e}^{-at} + \frac{b}{a};\ t = 1, 2, \ldots, n \quad (14)$$

We set $x^{(1)}(0) = x^{(0)}(1)$, then

$$\hat{x}^{(1)}(t+1) = (x^{(0)}(1) - \frac{b}{a})\mathrm{e}^{-at} + \frac{b}{a};\ t = 1, 2, \ldots, n \quad (15)$$

Finally, by restoring the accumulating generation, we can express the restored values of $\hat{x}^{(0)}(t+1)$ as

$$\hat{x}^{(0)}(t+1) = \hat{x}^{(1)}(t+1) - \hat{x}^{(1)}(t), t = 1, 2, \ldots, n \quad (16)$$

In a GM(1,1) model, the parameter a is known as the development coefficient, which describes the development states of $\hat{X}^{(1)}$ and $\hat{X}^{(0)}$ and indicates the dynamic characteristics of the system. The parameter b is called the gray action quantity, which reflects the effects of the environment that surrounds the system. In general, the variables that act on the system should be external or predetermined. However, GM(1,1) is a single-sequence model, which makes use of only the system's behavioral sequence (or the so-called output sequence or background values) without considering any externally acting sequences (or the so-called input sequences or driving quantities). The gray action quantity b in GM(1,1) is derived from the background values that reflect changes contained in the data whose exact connotation is gray. Therefore, this model does not need detailed information of the system and uses only the system's behavioral variants. It provides an effective way to build simulation models for complicated systems with very little data (Liu and Lin 1998; Liu et al. 2004).

Therefore, let $X^{(0)} = (x^{(0)}(1), x^{(0)}(2), \ldots, x^{(0)}(n))$ be an original spring discharge time series. Using the GM(1,1) model, we can obtain an estimate of the long-term trend, $\hat{x}^{(0)}(t)$.

Analysis of the Periodic Variation

The periodic variation is acquired by fitting the residuals of the long-term trend, $\hat{x}^{(0)}(t)$. The residuals are given by

$$\epsilon(t) = x^{(0)}(t) - \hat{x}^{(0)}(t) \quad (17)$$

We fit the residuals sinusoidally and obtain the periodic variation,

$$S(t_i) = A_i \sin \frac{2\pi t_i}{T_i} \qquad (18)$$

where i denotes different periods, $S(t_i)$ the simulation of the residuals in period i at time t, A_i considered as the amplitude of period i, and T_i is the length of period i.

When combining the long-term trend, $\hat{x}^{(0)}(t)$, and the periodic variation, $S(t_i)$, we get the long-term and periodic trend $TS(t)$:

$$TS(t) = \hat{x}^{(0)}(t) + S(t_i) \qquad (19)$$

The Calculation of Random Fluctuation

We calculated the random fluctuations as follows:

$$R(t) = x^{(0)}(t) - TS(t) \qquad (20)$$

Because of the unpredictability of the random factor, we use the mean absolute value of the random fluctuations, $\overline{|R(t)|}$, to take the place of $R(t)$ in Equation 1, so we have

$$Q(t) = \hat{x}^{(0)}(t) + S(t_i) \pm \overline{|R(t)|} \qquad (21)$$

Application of the Model

Hydrogeological Setting of the Liulin Springs Basin

The Liulin Springs complex is located in the Sanchuan River valley in the Liulin ground water basin located west of Shanxi Province (Figure 1). The spring complex consists of ~100 springs that are classified into five groups. The springs are distributed along 2 km of the river, and the ground surface elevation ranges from 790 to 801 m above sea level.

Between 1957 and 2004, the average spring discharge of the complex was 3.38 m^3/s, and the average precipitation over the complex was 506 mm. During this 48-year span, ~65% of the annual precipitation occurred during July, August, and September (Han et al. 1993). The Liulin ground water basin covers an area of 5100 km^2, ranging from 660 to 1200 m above sea level with the lowest elevation in the west. The northern and eastern boundaries of the basin are composed of Archaean metamorphic rock, while the southern and western boundaries consist of Carboniferous-Permian coal-bearing sandstone and shale (Figure 1). Karst ground water in the middle Ordovician carbonate aquifers moves toward the Liulin Springs complex.

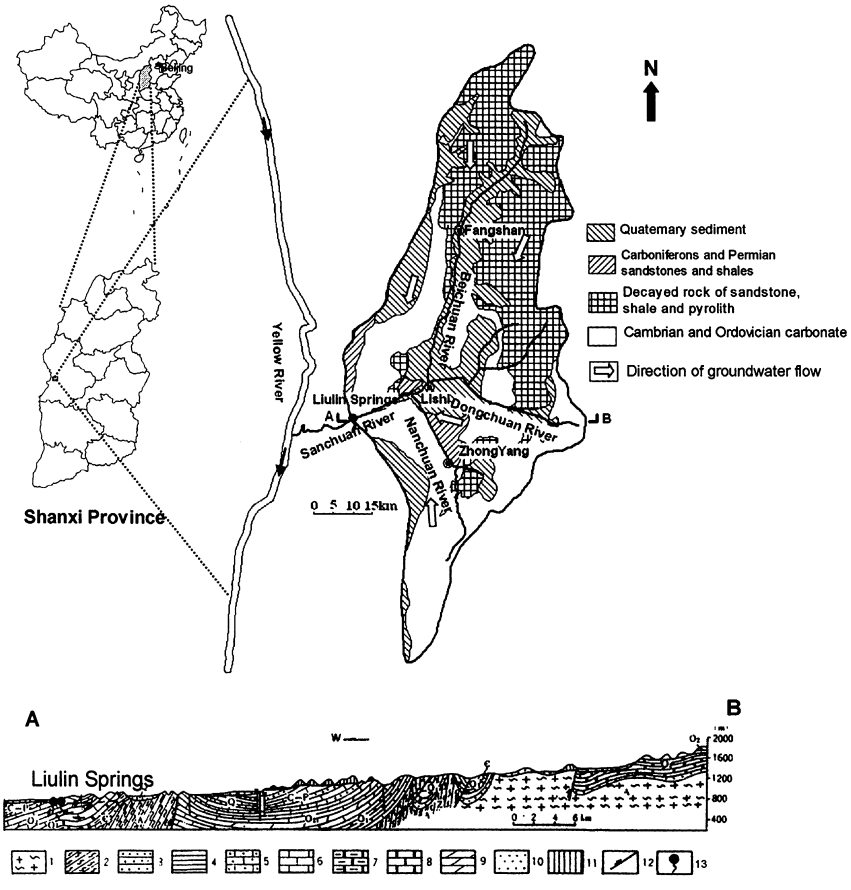

Figure 1. Location of the Liulin Springs, and a simplified hydrogeology map, with a cross-sectional geologic map of the Liulin Basin (Reprinted from Hao et al. 2006, with permission from Elsevier).

Ground water from the middle Ordovician karst aquifer has been one of the most important sources of water supply in northern China. The lithology of the aquifer is limestone and dolomite, with several thin layers or lenses of anhydrite sandwiched between carbonate aquifers. The anhydrite can be partly preserved under confined conditions only when the aquifers are overlain by thick, relatively impermeable Carboniferous-Permian coal-bearing sandstone and shale. Along the river channel where leakage occurs, the middle Ordovician carbonate either appears as outcrops or underlies alluvial sediments, creating favorable seepage conditions for the river water (Wang et al. 2001).

Since the early 1970s, the ground water resources of the basin have been developed for industrial, municipal, and irrigation uses. The continuous decline of spring flow has been attributed to the development of ground water resources. However, declining precipitation caused by climate change also contribute to declining spring flow (Guo et al. 2005).

Application of the Gray System Decomposition Model at the Liulin Springs Complex

In applying the gray system model as a predictive tool for future total Liulin Springs discharge, the postdevelopment period from 1973 to 2004 was deemed most representative of the ongoing development of karst ground water exploitation and the advent of drier conditions (Figure 2). We selected the average annual spring discharge sequence from 1973 to 2002 to set up the GM(1,1) model and selected data from 2003 to 2004 to calibrate the model. The spring discharge $X^{(0)}$ is the corrected discharge, which is calculated by adding the observed spring discharge to the rate of exploitation of karst ground water.

Using the corrected spring discharge data from 1973 to 2002, we set up the gray differential equation of the Liulin Springs discharge GM(1,1) model with these parameters:

$$\begin{pmatrix} a \\ b \end{pmatrix} = \begin{pmatrix} 0.0201 \\ 3.8762 \end{pmatrix} \tag{22}$$

The whitenizing equation of the GM(1,1) model is expressed as

$$\frac{dx^{(1)}(t)}{dt} + 0.0201x^{(1)}(t) = 3.8762 \tag{23}$$

and the approximate time response sequence is

$$\hat{x}^{(1)}(t+1) = -189.5678e^{-0.0201t} + 192.8578 \tag{24}$$

Finally, from restoration of the accumulating generation, the long-term trend of spring discharge is expressed as

$$\hat{x}^{(0)}(t+1) = \hat{x}^{(1)}(t+1) - \hat{x}^{(1)}(t),\ t = 1, 2, \ldots, n \tag{25}$$

Figure 3 shows the long-term trend curve of the Liulin Springs discharge from 1973 to 2002. The figure clearly illustrates that the long-term trend, $\hat{x}^{(0)}(t)$, is descending. The curve accurately reflects the general trend of the Liulin Springs discharge over time but does not correspond with its periodic fluctuation. In this curve, the average value of absolute residual error is $\overline{|\epsilon(t)|} = 0.241$ and the mean relative error $\overline{|q(t)|} = 7.7\%$.

In order to determine the periodic variation, $S(t_i)$, of the Liulin Springs, we fit the residual curve of the long-term trend sinusoidally (Figure 4). The amplitude of the sinusoid is estimated by the mean absolute value of the long-term trend residuals in i stage, $\overline{|\epsilon_i(t)|}$:

$$S(t_i) = \overline{|\epsilon_i(t)|}\sin\frac{2\pi t_i}{T_i} \tag{26}$$

According to the trends, the residual curve is divided into three phases. In the first phase, the period T_1 is 10 years from 1973 to 1983, and its amplitude is $\overline{|\epsilon_1(t)|} = 0.397$. In the second phase, the period T_2 is 16 years from 1983 to 1999, and its amplitude is $\overline{|\epsilon_2(t)|} = 0.356$. From stage 1 to stage 2 the periods become larger and the amplitude becomes smaller. Thus, we postulate that in stage 3, the period T_3 is 16 years, and its amplitude is the mean absolute the value of residual data from 1999 to 2002 $\overline{|\epsilon_3(t)|} = 0.120$.

The long-term and periodic trend, $TS(t)$, is obtained by combining the long-term trend, $\hat{x}^{(0)}(t)$, and the periodic variation, $S(t_i)$. The $TS(t)$ curve is displayed in Figure 3, which shows that the curve fits the discharge with a higher accuracy than the long-term trend curve. In the $TS(t)$ curve, the average absolute value of residual error is $\overline{|\epsilon'(t)|} = 0.153$ and the mean relative error $\overline{|q'(t)|} = 4.91\%$.

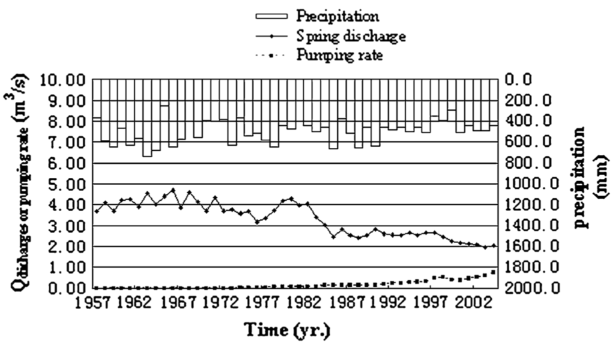

Figure 2. Change in spring discharge, pumping rate, and precipitation 1957 to 2004.

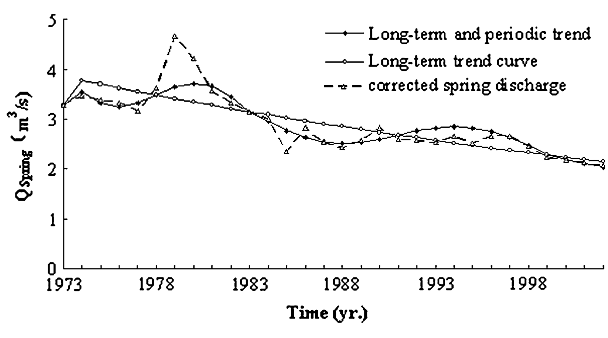

Figure 3. Gray model simulation curves for the Liulin Springs.

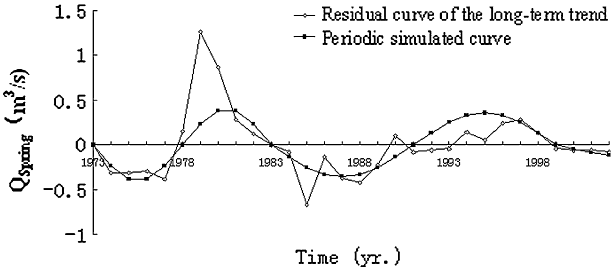

Figure 4. Periodic variation curves for the Liulin Springs.

According to Equation 20, the random fluctuation curve $R(t)$ is acquired, and its curve is shown in Figure 5. In stage 1, the average absolute value of random fluctuation is $\overline{|R_1(t)|} = 0.205$, $\overline{|R_2(t)|} = 0.134$ in stage 2, and $\overline{|R_3(t)|} = 0.028$ in stage 3. The random fluctuation values become smaller from stage 1 to stage 3, which is likely caused by annual average precipitation becoming less variable (Table 1) and human activities having a moderating effect on the fluctuation of karst ground water discharge. Notice that the time lag between precipitation and spring discharge (i.e., karst ground water residence time) is ~4 years at the Liulin Springs (Hao et al. 2006). Accordingly for each of the three phases, we used precipitation data starting 4 years prior to the beginning of each phase of spring flow, but for the same length of time for each phase of spring flow. For example, for the first phase of spring flow, which is 1973 to 1983, we used an 11-year precipitation data set that began 4 years prior to 1973, i.e., 1969 to 1979 (Table 1).

Accordingly, using Equation 21, we have predicted the spring discharges at the Liulin Springs from 2003 to 2010, and the results are listed in Table 2. The long-term trend, $\hat{x}^{(0)}(t)$, is predicted by Equations 24 and 25. Notice that while the prediction period is determined by stage 3, the periodic component, $S(t_i)$, is calculated by

$$S(t_3) = \overline{|\epsilon_3(t)|} \sin \frac{2\pi t_3}{T_3} \qquad (27)$$

and the random fluctuation component is given by $\overline{|R(t)|} = \overline{|R_3(t)|} = 0.028$. Finally, we obtain the predicted spring discharge according to Equation 21. The results are tabulated in Table 2.

The predicted spring discharges range from 1.958 to 2.014 m^3/s for 2003 and from 2.025 to 2.081 m^3/s for 2004. The recorded discharge at the Liulin Springs in 2003 and 2004 was 1.98 and 2.05 m^3/s, respectively. The relative errors of the predicted discharges range from −1.1% to 1.72% in 2003 and −1.51% to 1.22% in 2004.

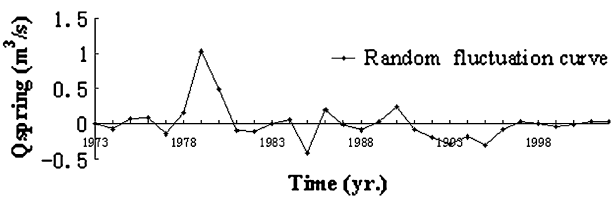

Figure 5. Random fluctuation curve for the Liulin Springs complex.

Table 1
The Annual Average Precipitation and Variance in Each Stage

Stages	Time	Annual Average Precipitation (mm)	Variance (mm^2)
1	1969–1979	494.0	10,706.5
2	1979–1995	491.6	7192.0
3	1995–2004	436.2	5120.6

Discussion and Conclusions

Gray system theory developed in the context of control system theory was adapted to analyze and predict the temporal variation of discharge from the karst aquifer in the Liulin ground water basin. Our analysis of the discharge data sets at the spring over different time scales indicates that the discharge data sets have several trends. We decompose spring discharge into three components: the long-term trend, $\hat{x}^{(0)}(t)$, periodic variation, $S(t_i)$, and random fluctuations, $R(t)$. We use the gray system GM(1,1) model to simulate the long-term trend. By analyzing the residuals of the long-term trend, we obtain periodic variation and random fluctuation components. Thus, the simulation model of karst spring discharge is based on the three time series components: a trend, a periodic component, and a random component. Application of the model to the Liulin Springs complex shows that the model performs well. The relative errors of the predicted discharges range from −1.1% to 1.72% for 2003 and −1.51% to 1.22% for 2004. The predicted results of spring discharge from 2003 to 2010 suggest that the Liulin Springs discharge will likely decrease over time, with small fluctuations.

Karst ground water development began in the early 1970s in the Liulin Springs basin. The development has undoubtedly altered the ground water flow regime, impacted the recharge of precipitation to the karst aquifer, and, in turn, caused the decrease of spring discharge. Figure 2 shows that since the 1970s, the exploitation has exhibited an increasing trend over the past 30 years, corresponding to economic and population growth. It thus appears that there is a clear connection between the reduction of spring discharge and the ground water exploitation. However, according to our analysis, before 1970 the average discharge of the Liulin Springs was found to be 4.17 m^3/s and the annual average precipitation was 546.1 mm. For the period from 1970 to 2004, the annual average discharge had dropped to 2.97 m^3/s and the annual average precipitation fell to 479.6 mm, a difference of 1.20 m^3/s for the spring discharge and 66.5 mm for the precipitation. The average pumping rate after 1970, however, was found to be 0.24 m^3/s. These findings lead us to conclude that climate change is more likely to be responsible for the decline of the spring discharge of the Liulin Springs, while human activities are the secondary factor. Meteorological records in North China also indicate a continuous decrease in precipitation over the region since the 1970s (Ma et al. 2004; Guo et al.

Table 2
Prediction of the Liulin Springs Discharge (in m^3/s)

Year	Long-Term Trend $\hat{x}^{(0)}(t)$	Periodic Variation $S(t)$	Long-Term and Periodic Trend TS(t)	Random Fluctuation $\overline{|R_3(t)|}$	Predicted Discharge $Q(t)$
2003	2.106	−0.120	1.986	0.028	1.958–2.014
2004	2.064	−0.011	2.053	0.028	2.025–2.081
2005	2.023	−0.085	1.938	0.028	1.910–1.966
2006	1.983	−0.046	1.937	0.028	1.909–1.965
2007	1.943	0	1.943	0.028	1.915–1.971
2008	1.905	−0.046	1.951	0.028	1.923–1.979
2009	1.867	0.085	1.952	0.028	1.924–1.980
2010	1.830	0.011	1.841	0.028	1.813–1.869

2005). On this basis, we suggest that continuous decline of karst ground water level and the corresponding decrease in spring discharge in North China might be largely a response of the ground water system to the decrease in regional precipitation rather than only the development of ground water resources.

Acknowledgments

The authors acknowledge the support of the National Natural Science Foundation of China (NSFC-40572150), the Fellowship of Shanxi Scholarship Council of China, and the Science and Technology Development Program of the Education Bureau of Shanxi Province. Thanks are extended to Dr. Sifeng Liu and Professor Xuemeng Wang for their comments in application of the gray system model. Many thanks are extended to Jimmy Jiao, Lee Florea, and an anonymous reviewer for their efforts reviewing the manuscript and their very encouraging, insightful, and constructive comments. The authors extend their gratitude to Joseph Stefani and Martha P.L. Whitaker for technical editing of the manuscript.

References

Barfield, B.J., G.K. Felton, E.W. Stevens, and M. McCann. 2004. A simple model of karst spring flow using modified NRCS procedures. *Journal of Hydrology* 287, no. 1–4: 34–48.

Deng, J. 1985. *Gray Control System* (in Chinese). Wuhan, China: Huazhong University of Science and Technology Press.

Deng, J. 1982. Control problems of gray systems. *Systems and Control Letters* 2, no. 5: 288–294.

Dreiss, S.J. 1982. Linear kernels for karst aquifers. *Water Resources Research* 18, no. 4: 865–876.

Guo, Q., Y. Wang, T. Ma, and L. Li. 2005. The variation of discharge from karst springs in recent 50 years in Shanxi Province, China. *Science in China: Series D Earth Sciences* 35, no. 2: 167–175.

Haliham, T., C.M. Wicks, and J.F. Engeln. 1998. Physical response of karst drainage basin to flood pulse: Example of the Devil's Icebox cave system (Missouri, USA). *Journal of Hydrology* 204, no. 1–4: 24–36.

Han, X., R. Lu, and Q. Li. 1993. *Karst Water System: A Study on Big Karst Springs in Shanxi* (in Chinese with English abstract). Beijing, China: Geological Publishing House.

Hao, Y., T.J. Yeh, Z. Gao, Y. Wang, and Y. Zhao. 2006. A gray system model for studying the response to climatic change: The Liulin karst springs, China. *Journal of Hydrology* 32, no. 3–4: 668–670.

He, Y., B. Han, C. Xue, and Y. He. 1997. *Study of Karstic-Water in China* (in Chinese with English abstract). Shanghai, China: Tongji University Press.

Labat, D., R. Ababou, and A. Mangin. 2000. Rainfall-runoff relations for karstic springs. Part I: Convolution and spectral analysis. *Journal of Hydrology* 238, no. 3–4: 123–148.

Labat, D., R. Ababou, and A. Mangin. 1999. Linear and nonlinear input/output models for karstic spring flow and flood prediction at different time scales. *Stochastic Environmental Research and Risk Assessment* 13, no. 5: 337–364.

Lee, R., and R. Wang. 1998. Parameter estimation with color noise effect for differential hydrological gray model. *Journal of Hydrology* 208, no. 1–2: 1–15.

Liu S., Y. Dang, and Z. Fang. 2004. *Gray System Theory and Application* (in Chinese) . Beijing, China: Science Press.

Liu, S., and Y. Lin. 1998. *An Introduction to Gray System: Foundations, Methodology and Applications*. Slippery Rock, Pennsylvania: IIGSS Academic Publisher.

Long, A.J., and R.G. Derickson. 1999. Linear system analysis in a karst aquifer. *Journal of Hydrology* 219, no. 3–4: 206–217.

Ma, T., Y. Wang, and Q. Guo. 2004. Response of carbonate aquifer to climate change in northern China: A case study at the Shentou Springs. *Journal of Hydrology* 297, no. 1–4: 274–284.

Majone, B., A. Bellina, and A. Borsatob. 2004. Runoff generation in karst catchments: Multifractal analysis. *Journal of Hydrology* 294, no. 1–3: 176–195.

Quinlan, J.F., G.J. Davies, S.W. Jones, and P.W. Huntoon. 1996. The application of numerical models to adequately characterize ground-water flow in karstic and other triple-porosity aquifers. In *Subsurface Fluid-Flow Modeling, ASTM STP 1288, American Society for Testing and Materials*, ed. J.D. Ritchy and J.O. Rumbaugh, 114–133. West Conshohocken, Pennsylvania: ASTM.

Scanlon, B.R., R.E. Mace, M.E. Barrett, and B. Smith. 2003. Can we simulate regional ground water flow in a karst system using equivalent porous media models? Case study, Barton Springs Edwards aquifer, USA. *Journal of Hydrology* 276, no. 1–4: 137–158.

Wang, Y., T. Ma, and Z. Luo. 2001. Geostatistical and geochemical analysis of surface water leakage into groundwater on a regional scale: A case study in the Liulin karst system, northwestern China. *Journal of Hydrology* 246, no. 1–4: 223–234.

White, W.B. 2002. Karst hydrology: Recent developments and open questions. *Engineering Geology* 65, no. 2–3: 85–105.

White, W.B. 1988. *Geomorphology and Hydrology of Karst Terrains*. New York: Oxford University Press.

Xia, J. 2000. *Gray System Hydrology: Theory, Methodology and Application* (in Chinese). Wuhan, China: Huazhong University of Science and Technology Press.

Yuan, D.X. 1994. *Karstology of China* (in Chinese). Beijing, China: Geological Publishing House.

Zhang, Y., E. Bai, R. Libra, R. Rowden, and H. Liu. 1996. Simulation of spring discharge from a limestone aquifer in Iowa. *Hydrogeology Journal* 4, no. 4: 41–54.